23 June 2000

ELSEVIER

Chemical Physics Letters 323 (2000) 474–481

CHEMICAL PHYSICS LETTERS

www.elsevier.nl/locate/cplett

Intramolecular motion in dibenzobarrelenephosphinyl radical: a single crystal EPR study at variable temperature

Marcin Brynda, Théo Berclaz, Michel Geoffroy *

Department of Physical Chemistry, University of Geneva, 30 Quai Ernest Ansermet, 1211 Geneva, Switzerland

Received 7 October 1999; in final form 11 April 2000

Abstract

The g, ^{31}P and ^{1}H hyperfine tensors of the dibenzobarrelene phosphinyl radical, trapped in an X-irradiated single crystal of dibenzobarrelene phosphine, were estimated at 45 and 300 K. They indicate that among the three locations of the phosphinyl hydrogen expected from DFT calculations, only two are occupied at 40 K and that the third one remains practically vacant, even at 300 K. The temperature dependence of the EPR spectrum was simulated by assuming jumps between two P–H bond orientations (energy barrier $\cong 0.5$ kcal mol^{-1}) which correspond to the conformation of the PH_2 moiety in the only rotamer present in the dibenzobarrelene phosphine crystal.

1. Introduction

Because most chemical processes involve local changes in molecular structures, the study of intramolecular motions has always been of crucial interest for chemists [1,2]. This interest has continued to increase in recent years, as these phenomena can be used for developing molecular devices [3]. We have recently shown that X-irradiation of single crystals of triptycene derivatives, bearing a phosphine group in the C_9 position (e.g. **1**), leads to the trapping of a phosphinyl radical whose P–H bond undergoes a temperature dependent rotation around the P–C axis [4]. This motion, which corresponds to jumps between three configurations, can be more or less affected by the presence of large substituting groups on the barrelene skeleton [5]. For example, whereas the P–H motion is blocked at 110 K for **2**, it continues further to 100 K for **1**. The recent synthesis [6] of **3**, the only primary phosphine with an ethylenic bond in the β-position which forms air-stable single crystals at room temperature, now makes possible investigations on a system bearing no substituent on C_8. In the present Letter, we show that suppression of steric constraints along one of the

* Corresponding author. Fax: +22-702-61-03; e-mail: michel.geoffroy@chiphy.unige.ch

0009-2614/00/$ - see front matter
PII: S0009-2614(00)00525-X

barrelene C–C bonds not only affects the temperature at which the motion is blocked, but, also drastically changes the nature of the intramolecular motion.

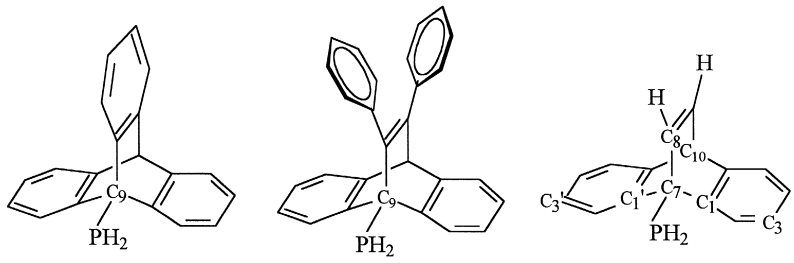

1 **2** **3**

2. Experimental

2.1. Compound and irradiation

3 was synthesized [6] by reacting PCl_3 with the Li-derivative of dibenzobarrelene and by subsequent reduction with $LiAlH_4$. The starting compound (bromodibenzobarrelene) was obtained by heating, in a sealed glass tube, a furan-dimethyl acetylene dicarboxylate adduct in the presence of 9-bromoanthracene. The crystal structure of **3** is known [6]: orthorhombic, *Pnma*. Large single crystals (mp 108°C) were grown by slow evaporation of a solution in hexane/ether (9:1); after indexation of their faces, they were oriented on a sample holder, exposed for 2 h to the radiation of a Philips X-ray tube (tungsten anticathode, 30 mA, 30 kV, room temperature) and finally coated with an inert polymer in order to avoid reaction with air or humidity. The sample holder was designed in order to align the EPR reference axes OX, OY, OZ along the crystallographic axes *b*, *a* and $-c$, respectively.

2.2. DFT calculations

Calculations were performed with the GAUSSIAN 94 [7] package on a Hewlett Packard Convex Exemplar. DFT calculations [8] were carried out at the B3LYP/3-21G* level

2.3. EPR study

2.3.1. Instrumentation and tensors determination

EPR spectra were recorded on a Bruker 300 spectrometer (X-band, 100 KHz field modulation) equipped with an ITC503 Oxford cryostat allowing measurements between 4 and 300 K.

The angular variation of the signals was analysed using a Hamiltonian which takes the electronic and nuclear Zeeman interactions as well as the hyperfine couplings with a proton and a ^{31}P nucleus into account. The elements of these three tensors were determined by using an optimisation program, based on the algorithm of Levenberg–Marquardt [9], which compares the position of the experimental resonance lines with those calculated by second order perturbation theory.

2.3.2. Temperature dependence of the spectra

The temperature dependence of the EPR spectra was analysed, for a given orientation of the magnetic field, by determining the values of the exchange parameters k_{ij}, between sites *i* and *j*, which lead to the best simulations of the experimental spectra. These simulations were performed by means of the method already used for the study of phosphinyl radicals trapped in **1** [4] and **2** [5]; the calculations use the density matrix formalism and are based on the same concepts as those used by other authors [10–12]. They were performed in the Liouville space and the spectrum was obtained as the sum of the

elements of the vector $\rho^{-+} = i\mathbf{I}_0(\mathbf{U}^{-1}\mathbf{\Lambda}\mathbf{U} - i\omega\mathbf{1})^{-1} P$. The **U** and **Λ** matrices are built, respectively, from the eigenvectors and eigenvalues of a matrix whose diagonal elements contain the transition positions, the inverse of the relaxation time T_2 and the sum of exchange parameters k_{ij}, while the non-diagonal elements correspond to the appropriate k parameter.

3. Results

3.1. EPR spectra

A typical EPR spectrum obtained at 40 K with an X-irradiated single crystal of **3** is shown in Fig. 1a. It is characterised by a large ^{31}P hyperfine splitting (> 12.3 mT) and a smaller coupling with a proton (1.5 mT). Two magnetically non-equivalent orientations of the radical are present in the crystal and lead to two sets of signals marked I and J, respectively. The additional small signal K is isotropic; it probably results from a radical centred on the C_{10} carbon and will not be considered here. The temperature dependence of the spectrum recorded between 40 and 300 K for the same orientation of the magnetic field is also shown in Fig. 1a. The modifications are reversible and reveal a dynamical process. The angular variations of the signals recorded both at low and room temperatures are shown in Fig. 2. Their analysis leads to the tensors given in Tables 1 and 2. Due to the large anisotropy of the ^{31}P coupling, the corresponding eigenvectors are determined with a very good accuracy whereas the precision on the ^{1}H eigenvectors is rather poor.

We will first examine the EPR parameters measured at 45 K. Decomposition of the ^{31}P hyperfine tensor into isotropic and anisotropic coupling constants, leads, on the hypothesis of three positive

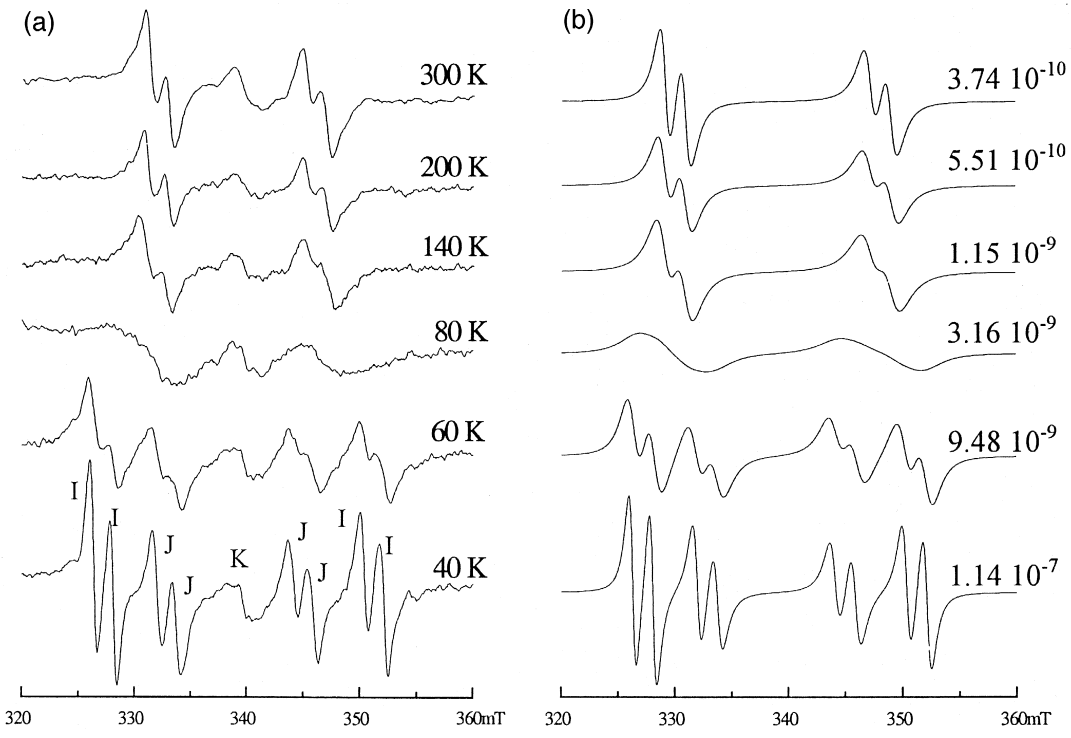

Fig. 1. (a) Temperature dependence of the EPR spectra obtained with an X-irradiated single crystal of **3** (H_0 in the *ab* plane, 20° from the axis *a*). (b) Simulated spectra (with the corresponding exchange rate constant (in s^{-1})).

eigenvalues, to the values reported in Table 3; the spin densities are obtained by comparing these parameters with the atomic coupling constants [13] ($A^*_{iso} = 13\,300$ MHz, $2B_0 = 733$ MHz): $\rho_s = 0.02$ and $\rho_p = 0.73$. These parameters are consistent with a phosphinyl radical; moreover the ^{1}H hyperfine constants (Table 3), calculated by assuming three negative eigenvalues are in accord with the values expected for the hydrogen atom of a RPH radical. The ^{31}P-$T_{\|}$ direction, which is expected to be aligned along the phosphorus p-orbital containing the unpaired electron, makes an angle of 94° with the

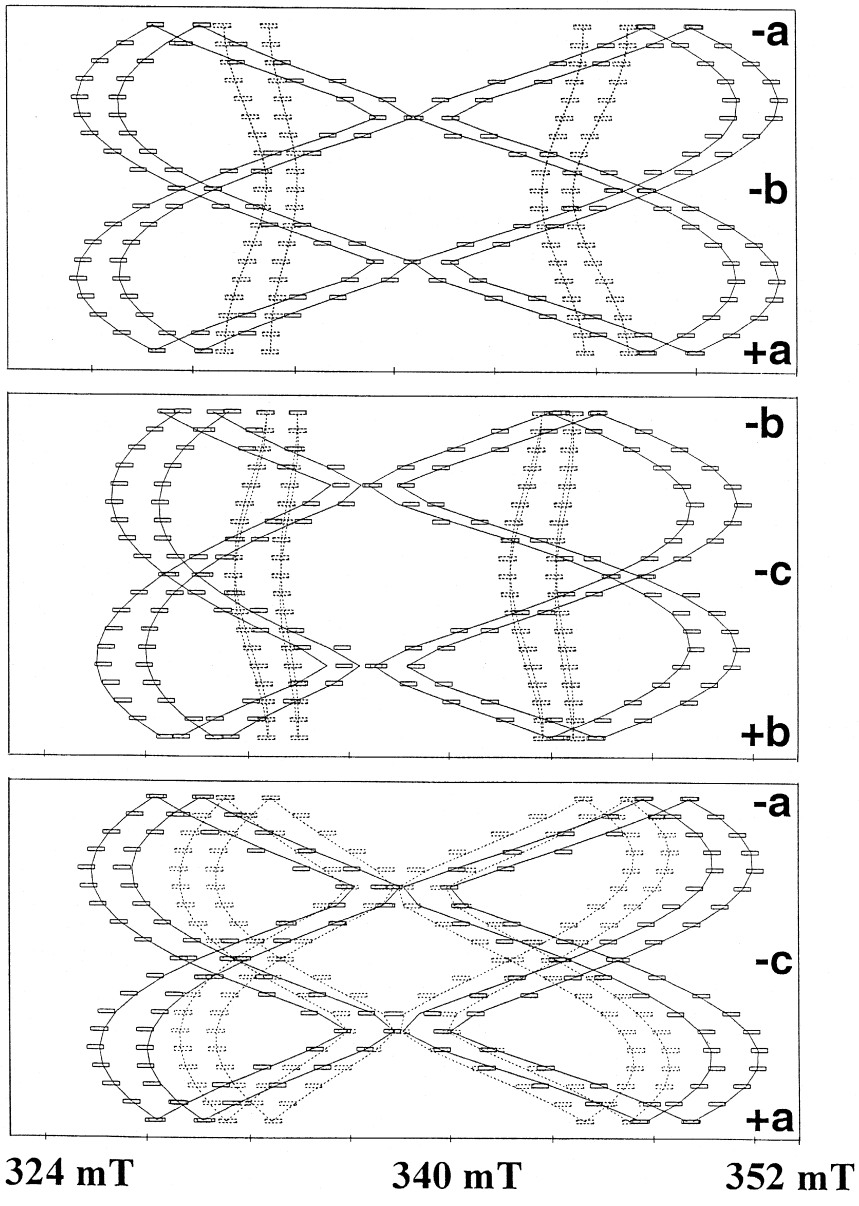

Fig. 2. Angular variation of the EPR signals obtained with an X-irradiated single crystal of **3**: (—) at 45 K, (. . .) at 300 K.

Table 1
EPR tensors obtained at 45 K with an X-irradiated single crystal of **3**

Tensor	Principal values	Direction cosines[a]		
		λ	μ	ν
g	2.0032	−0.7683	0.3634	−0.5270
	2.0083	0.3952	0.9169	0.0560
	2.0160	0.5035	−0.1652	−0.8480
^{31}P coupling [b]	842	0.5769	−0.6454	0.5006
	52	−0.1203	−0.6734	−0.7294
	11	0.8079	0.3606	−0.4662
^{1}H coupling [b]	(−)54	−0.6710	−0.3154	−0.6711
	(−)42	−0.0966	−0.7352	−0.6710
	(−)16	0.9345	0.1650	0.6575

[a] Other orientations of the radical: $-\lambda, \mu, \nu$; $\lambda, -\mu, \nu$; $\lambda, \mu, -\nu$.
[b] In MHz.

crystallographic P–C_7 bond direction, consistent with the trapping of radical **4**.

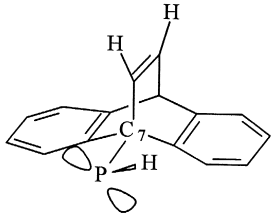

radical **4**

The crystal structure of **3** shows that in the undamaged molecule, the molecular symmetry plane

Table 2
EPR tensors obtained at 300 K with an X-irradiated single crystal of **3**

Tensor	Principal values	Direction cosines[a]		
		λ	μ	ν
g	2.0027	0.1713	0.9542	0.2452
	2.0048	−0.9789	0.1368	0.1515
	2.0113	−0.1111	0.2659	−0.9576
^{31}P coupling [b]	504	−0.0042	−0.7932	−0.6090
	308	−0.9999	0.0001	0.0068
	49	0.0054	−0.6090	0.7931
^{1}H coupling [b]	(−)55	0.2005	−0.6064	−0.7694
	(−)45	−0.3208	0.7827	0.5333
	(−)32	0.9257	−0.1399	0.3515

[a] Other orientations of the radical are given: $-\lambda, \mu, \nu$; $\lambda, -\mu, \nu$; $\lambda, \mu, -\nu$.
[b] In MHz.

Table 3
Hyperfine coupling constants (MHz) for **4**

		Isotropic	Anisotropic		
^{31}P	experimental	302	540	−250	−290
	calculated	120	547	−265	−283
^{1}H	experimental	−37	+21	−4	−17
	calculated	−33	+16	+1	−17

lies in the *ac* plane. In accordance with the orthorhombic structure of the crystal, two different sets of curves are obtained in each EPR reference plane at 45 K, whereas, at room temperature, two sets are distinguishable only in the *YZ* plane. Since the anisotropy of the spectrum is principally governed by the large anisotropy of the ^{31}P coupling, this suggests that, at 300 K, a dynamic process leads to a ^{31}P tensor which has one of its eigenvectors aligned along the *b*-axis. This is confirmed by the EPR parameters shown in Table 2; they indicate that, at room temperature, the ^{31}P hyperfine tensor has lost its axial symmetry and that the eigenvectors associated with the maximum and minimum couplings lie in the *YZ* plane. At low temperature, a molecule of dibenzobarrelene phosphine **3** therefore gives rise to the radical **4** whose magnetic phosphorus p-orbital is aligned either along the $T_{\|a}(\lambda, \mu, \nu)$ direction or along the $T_{\|b}(-\lambda, \mu, \nu)$ direction. The angle formed by these two directions is equal to 70° and its bisector is aligned along the ^{31}P-T_{max} eigenvector measured, at room temperature, for the averaged structure. Furthermore the $T_{\|a}$ direction makes an angle of 5° with the normal n_1 to the crystallographic

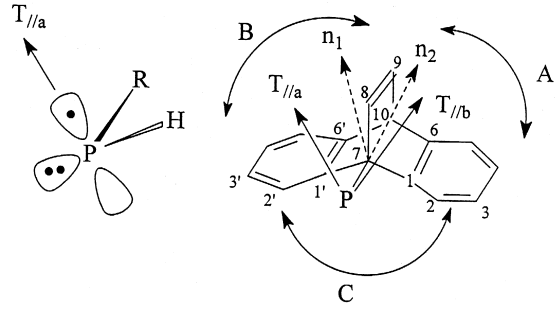

Fig. 3. Orientation of the ^{31}P hyperfine coupling in the dibenzobarrelene phosphine framework (n_1 and n_2 are perpendicular to the crystallographic $C_1'C_7P$ and C_1C_7P planes, respectively).

C'_1C_7P plane, while $T_{\|b}$ makes the same angle with the normal n_2 to the C_1C_7P plane. As shown in Fig. 3, this implies that, at 45 K, the P–H bond of the radical **4** is located either in the sector A (defined by the two planes $C_7C_8C_9C_{10}$ and $C_7C_1C_6C_{10}$) or in the sector B (defined by the $C_7C_8C_9C_{10}$ and $C_7C'_1C'_6C_{10}$ planes).

4. DFT calculations

A full optimisation of the geometry of **4** indicates that the most stable rotamers correspond to the two staggered conformations $C_1C_7PH = 176.7°$(or $C'_1C_7PH = 176.7°$). The angle between the $C'_1C_7C_{10}$ and $C_1C_7C_{10}$ planes is equal to 118° and the torsion angle C_8C_7PH is equal to 57.4°. It is worthwhile mentioning that the phosphorus atom is very slightly out of the $C_7C_8C_9C_{10}$ symmetry plane of the barrelene ($C_1C_7P = 113.8°$, $C'_1C_7P = 115.5°$). The anisotropic coupling constants (Table 3) are in very good accord with the experimental values determined at 45 K, The agreement with the ^{31}P–Fermi contact interaction is much less satisfactory; this is not unexpected, the DFT predictions of ^{31}P-A_{iso} are generally rather poor when, as for a phosphinyl radical, this coupling essentially results from inner shell polarisation [14].

The variation of the potential energy of **4** with the C_8C_7PH torsion angle was calculated by keeping constant the geometry of the dibenzobarrelene skeleton, previously optimised for C_8C_7PH, equal to 60°. The resulting curve is shown in Fig. 4. The three minima correspond to staggered conformations. The lowest energy, E_{min}, found for the conformations A and B, is only 0.5 kcal mol^{-1} inferior to the value calculated for conformation C. The energy barrier to rotation between A and B is clearly smaller (1.5 kcal mol^{-1}) than that between A (or B) and C (5.5 kcal mol^{-1}). Optimisations of the geometry of **4** were also performed by relaxing all the parameters for C_8C_7PH equal to 0°, 60°, 120° and 180°. The energy of the molecule was less affected by this relaxation but the dihedral angle ξ between the $C_1C_7C_{10}$ and $C'_1C_7C_{10}$ planes was shown to slightly vary with the orientation of the P–H bond ($\xi = 117°$, 119° and 123° for $C_8C_7PH = 0°$, 60° and 120°, respectively), and to remain larger than the crystallographic value measured on **3** (113.8°). Moreover, the C_8C_7P angle which is equal to 115.5° in **3**, varies between 108.9° and 115.7° in the range $0 < C_8C_7PH < 120°$.

The calculated hyperfine couplings are practically invariant with the orientation of the P–H bond.

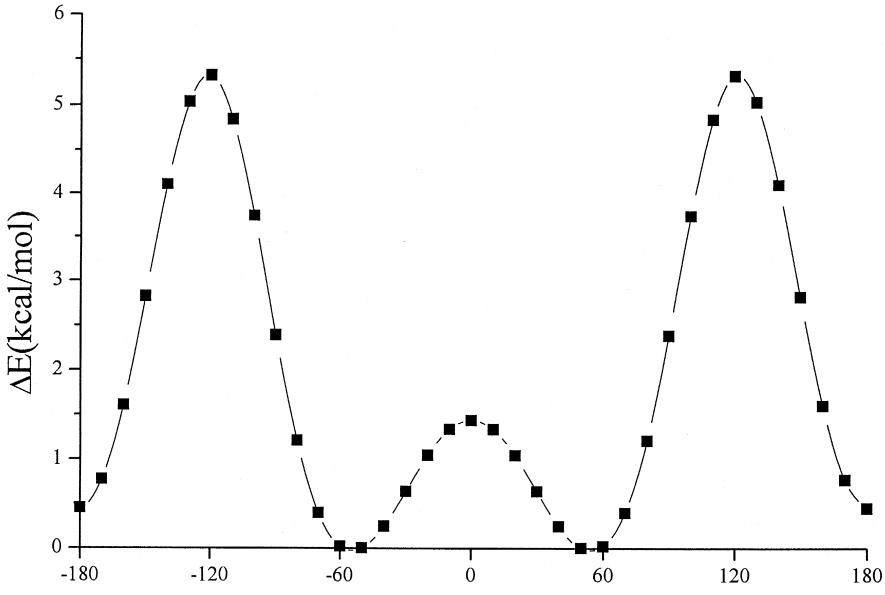

Fig. 4. DFT variation of the energy of radical **4** with the orientation of the P–H bond (C_8C_7PH dihedral angle).

5. Discussion

5.1. Orientations of the P–H bond at 45 and 300 K

At 45 K, the EPR spectra show that, in **4**, the rotation of the P–H bond around the C_7–P bond is blocked and that only the rotamers corresponding to the two staggered conformations A and B ($C_1C_7PH = C'_1C_7PH$ close to 180°) are detected. The third staggered conformation (magnetic phosphorus orbital perpendicular to the C_8C_7P plane) is not observed. Increasing the temperature provokes jumps between conformations A and B, and an averaging of the EPR tensors. The ^{31}P isotropic coupling constant is slightly larger at 45 K than at room temperature; this small difference (15 MHz) does not seem to be caused by a variation in the crystal lattice since the cell parameters have been shown to hardly vary with temperature. Perhaps it reflects a small distortion in the motion of the CPH group, in accord with the DFT calculations which show that the C_8C_7P and ξ angles slightly vary with the orientation of the P–H bond so that the phosphorus atom does not remain exactly in the barrelene symmetry plane.

5.2. Motion of the P–H bond between 45 and 300 K

Jumps between the two sites A and B modify the shape of the EPR spectra. The temperature dependence of the exchange rate constant k_{AB} was determined by simulating the spectra at various temperatures. (Fig. 1b). These simulations, obtained for several orientations of the magnetic field lead to the variation curve of k_{AB} versus T^{-1} shown in Fig. 5. This dependence is in accordance with the Arrhenius law and corresponds to an activation energy of 0.51 kcal mol^{-1}. This barrier to rotation is slightly lower than the value obtained from DFT calculations ($\Delta E = 1.5$ kcal mol^{-1}). Although DFT predicts only a small energy difference between sites A (or B) and C, and a moderate energy barriers (5.6 kcal mol^{-1}) between sites A and C (or B and C) we never detected any contribution of the site C. We calculated the expected positions of the resonance lines of the isolated C site and simulated the spectrum resulting from the exchange between the three sites A, B and C. At least for a temperature below 90 K, a population number for C equal to about 0.05 would drastically modify the simulated spectrum; above this temperature the rapid exchange between sites A

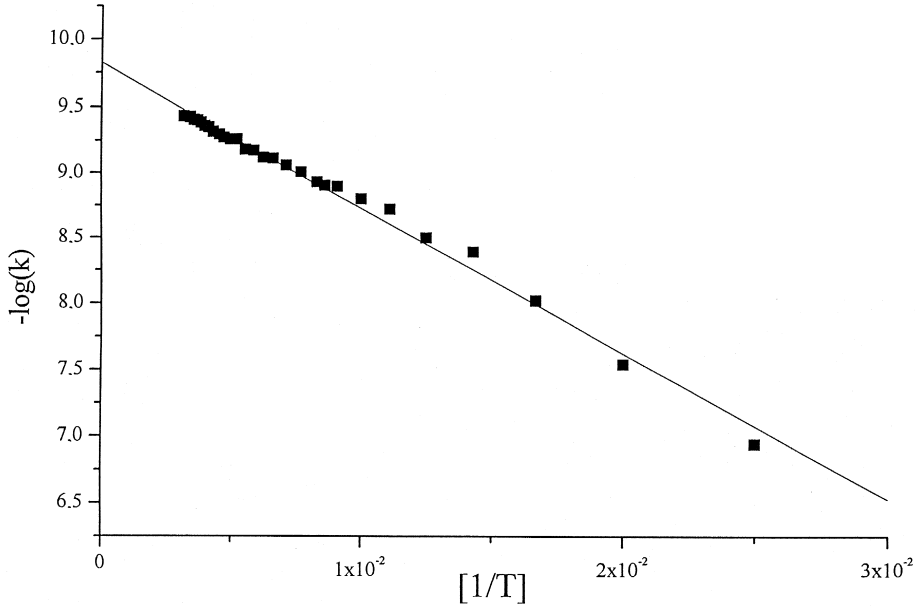

Fig. 5. Variation of the exchange rate constant k_{AB} with temperature.

and B makes the spectrum less sensitive to a participation of a third site. Moreover, a participation of site C in the P–H motion would increase the intermediate eigenvalue of the averaged ^{31}P hyperfine tensor in conflict with the tensor measured at 300 K.

It is worthwhile noting the parallelism between the behaviour of the phosphine and that of the corresponding phosphinyl radical: the crystal structure showed that for **1** the three hydrogen sites (P–H in the region A, B, C) were equally occupied, whereas the corresponding occupation numbers were equal to 0.8, 0.8 and 0.4 for **2** and that, in **3**, the position C remained vacant. Similarly, for the triptycenephosphinyl radical [4] the $^{\cdot}$P–H jumped between three equally populated sites whereas for the radical derived from **2** [5] the exchange occurred between three sites, one of which was appreciably less populated; finally, for **4** the phosphinyl hydrogen hops between two positions only.

6. Conclusion

The internal motion of a $^{\cdot}$P–H moiety around a C–$^{\cdot}$P bond (where C is an sp^3-hybridized carbon atom) is particularly sensitive to the intramolecular environment. In the dibenzobarrelene phosphinyl radical, only two of the three available sites are occupied by the phosphinyl hydrogen at low temperature ($40 < T < 90$ K). In this temperature range, the P–H group does not undergo a rotation around the C–P bond but hops between the two sites which are not located in the molecular symmetry plane.

Acknowledgements

We thank the Swiss National Fund for its financial support and the Crystallographic Laboratory (Dr. R. Cerny) for the measurement of the cell parameters at various temperatures.

References

[1] W.J. Orville-Thomas (Ed.), Internal Rotation in Molecules, Wiley, London, 1974.
[2] M. Oki, Acc. Chem. Res. 23 (1990) 351.
[3] T.R. Kelly, M.C. Bowyer, K.V. Bhaskar, D. Bebbington, A. Garcia, F. Lang, M.H. Kim, M.P. Jette, J. Am. Chem. Soc. 116 (1994) 3657.
[4] G. Ramakrishnan, A. Jouaiti, M. Geoffroy, G. Bernardinelli, J. Phys. Chem. 100 (1996) 10861.
[5] M. Brynda, T. Berclaz, M. Geoffroy, G. Ramakrishnan, G. Bernardinelli, J. Phys. Chem. 102 (1998) 8245.
[6] M. Brynda, M. Geoffroy, G. Bernardinelli, Chem. Commun. (1999) 961.
[7] M.J. Frisch et al., GAUSSIAN 94, Revision B.1, Gaussian, Pittsburgh, PA, 1995.
[8] A.D. Becke, J. Chem. Phys. 98 (1993) 5648.
[9] E. Soulié, T. Berclaz, M. Geoffroy, in: F. Bernardi, J.-L. Rivail (Eds.), AIP Conference Proceedings 330, Computational Chemistry, 1996, p. 627.
[10] J. Heinzer, J. Mol. Phys. 22 (1971) 167.
[11] C.M. Bogan, L.D. Kispert, J. Chem. Phys. 57 (1972) 3109.
[12] N.P. Benetis, L. Sjökist, A. Lund, J. Maruani, J. Magn. Reson. 95 (1991) 523.
[13] J.R. Morton, K.F. Preston, J. Magn. Reson. 30 (1978) 577.
[14] M. Chentit, H. Sidorenkova, M. Geoffroy, Y. Ellinger, J. Phys. Chem. 102 (1998) 10469.